



Published in final edited form as:

Analyst. 2014 May 7; 139(9): 2127–2132. doi:10.1039/c4an00230j.

## Rational Selection of Substrates to Improve Color Intensity and Uniformity on Microfluidic Paper-Based Analytical Devices

Elizabeth Evans<sup>a</sup>, Ellen Flávia Moreira Gabriel<sup>b</sup>, Wendell Karlos Tomazelli Coltro<sup>b</sup>, and Carlos D. Garcia<sup>a,1</sup>

<sup>a</sup>Department of Chemistry, The University of Texas at San Antonio, One UTSA Circle, San Antonio, TX 78249, USA

<sup>b</sup>Instituto de Química, Universidade Federal de Goiás, Campus Samambaia, Goiania, GO, 74001-970, Brazil

### Abstract

A systematic investigation was conducted to study the effect of paper type on the analytical performance of a series of microfluidic paper-based analytical devices (μPADs) fabricated using a CO<sub>2</sub> laser engraver. Samples included three different grades of Whatman chromatography paper, and three grades of Whatman filter paper. According to the data collected and the characterization performed, different papers offer a wide range of flow rate, thickness, and pore size. After optimizing the channel widths on the μPAD, the focus of this study was directed towards the color intensity and color uniformity formed during a colorimetric enzymatic reaction. According to the results herein described, the type of paper and the volume of reagents dispensed in each detection zone can determine the color intensity and uniformity. Therefore, the objective of this communication is to provide rational guidelines for the selection of paper substrates for the fabrication of μPADs.

### 1. Introduction

Since the development of the first microfluidic paper-based analytical device (μPAD) by Whitesides' group,<sup>1</sup> great progress has been made to improve the performance and number of applications of these devices. μPADs offer a low cost, portability, and a simple way to perform a variety of bioassays with minimal sample and reagent volumes. Recent publications have described the possibility of adapting this platform in the fabrication of three-dimensional devices,<sup>2</sup> bioactive papers,<sup>3</sup> built-in time delays,<sup>4</sup> and biofuel cells.<sup>5, 6</sup> Multiple procedures have been reported for making these devices, including photolithographic printing,<sup>7</sup> wax printing,<sup>8</sup> toner or inkjet printing,<sup>9</sup> flexographic printing,<sup>10</sup> plasma etching,<sup>11</sup> knife plotting,<sup>12,13</sup> and laser cutting.<sup>14</sup> This versatility has also been extended to the detection step, where a variety of detection methods (colorimetric,<sup>15</sup> electrochemical,<sup>16</sup> chemiluminescence,<sup>17</sup> and fluorescence<sup>18</sup>) have been implemented. Since it provides a low cost and semi-quantitative measurement (visual comparison with a colored scale), colorimetric detection is one of the most common detection modes used to

<sup>1</sup>To whom correspondence should be addressed: carlos.garcia@utsa.edu; Tel: +1 (210) 458-5774; Fax: +1 (210) 458-7428.

demonstrate the capability of  $\mu$ PADs performing clinical or diagnostic assays. This detection method can be further improved when a calibration curve (obtained with the aid of a scanner or a digital camera) is used, therefore minimizing the need of specific instrumentation.<sup>19</sup> These advantages have enabled the use of colorimetric  $\mu$ PADs for the analysis of glucose,<sup>20</sup> nitrite,<sup>15</sup> lactate,<sup>21</sup> uric acid,<sup>21</sup> proteins,<sup>22</sup> and others analytes.<sup>23, 24</sup>

Considering that the capabilities and applications of  $\mu$ PADs are rapidly expanding, an adequate selection of the type of paper used seems to be critical. Although most groups state they selected a particular paper because it allows for the detection color, a literature survey revealed that additional criteria for specific selection are not always stated. The six papers selected for the study were Whatman grade 1 filter paper (Grade 1F), Whatman grade 3 filter paper (Grade 3F), Whatman grade 4 filter paper (Grade 4F), Whatman grade 1 chromatography paper (Grade 1 CHR), Whatman grade 3MM chromatography paper (Grade 3MM CHR), and Whatman grade 4 chromatography paper (Grade 4 CHR). The chemical composition of the six substrates is >98% cellulose (see Supplementary Information). For example, grade 1 CHR paper has been selected in previous experiments due to its low-cost, hydrophilic character, availability, biocompatibility, homogeneity and wicking properties.<sup>8,9, 25, 26</sup> In addition, other paper substrates, including grade 3MM CHR,<sup>27</sup> as well as Whatman quantitative filter paper grade 1,<sup>28–30</sup> and grade 4<sup>31</sup> have been used without specifically addressing additional considerations. Since substrates can display a range in properties (see nominal specifications in Table 1) these findings suggest that a rational selection of the paper could significantly improve the performance of these devices when used for a particular application.

More specifically, the hypothesis of this work is that the differences in properties for each paper can affect the rate at which the sample moves towards the detection zones through the fluidic channels, can be optimized to control the reaction time, minimize the displacement of reagents, and yield a more uniform colorimetric response in the detection zones (5mm circles at the end of the channels where the enzymatic reaction takes place). Such color gradient in the detection zone has been identified as one of the major drawbacks affecting the applicability of  $\mu$ PADs.<sup>19</sup> To address this issue, a series of devices were fabricated using different types of paper and used to evaluate the color intensity and homogeneity. As a model system that would allow comparing the results of our strategy with previous reports, glucose was selected as the target analyte. In comparison with pH and total protein assays, the analysis of glucose often results in large color gradients in the sensing areas, forcing users to perform signal averaging or to measure the color intensity in a small area of the detection zone.<sup>32</sup>

## 2. Material and Methods

### 2.1. Reagents

All chemicals used in the experiment were analytical grade and used as received.  $\alpha$ -D-Glucose, A.C.S. reagent grade, glucose oxidase (GOx) from *Aspergillus niger* and horseradish peroxidase (HRP) were purchased from Sigma-Aldrich (St. Louis, MO). Potassium iodide was obtained from EM Science (Gibbstown, NJ). D-(+)-trehalose anhydrous was obtained from Tokyo Chemical Industry (Philadelphia, PA). Sodium

phosphate monobasic anhydrous and sodium phosphate dibasic anhydrous were acquired from Fisher Scientific (Waltham, MA). All solutions were made in ultrapure water ( $18\text{ M}\Omega\text{ cm}^{-1}$ , Barnstead Nanopure; Dubuque, IA). The paper substrates selected for these experiments (see Table 1) were purchased from Whatman (Maidstone, Kent, UK).

## 2.2. Instrumentation

A Legend Mini24 CO<sub>2</sub> Laser System (Epilog Laser Systems; Golden, CO, USA) was utilized to cut the paper-based analytical devices. This technique is an attractive alternative because it is a fast and reproducible, one-step procedure to make  $\mu$ PADs from a design produced in commercially available software. Moreover, since the machine uses a CO<sub>2</sub> laser (wavelength of  $10.6\text{ }\mu\text{m}$ ) to cut the paper, the edge of the paper is ablated creating a hydrophobic boundary.<sup>14</sup> Although a detailed description of the capabilities of the instrument can be found elsewhere,<sup>33</sup> all  $\mu$ PADs used in the experiments herein described were cut using the vector mode, at 30% speed (of a maximum linear speed of  $1.65\text{ cm}\cdot\text{s}^{-1}$ ) and 30% power (of a maximum intensity of 30 W). In order to minimize the possibility of ignition<sup>2</sup> of the paper inside the engraver, the engraving head was constantly used to impinge a stream of N<sub>2</sub> (house line) on the engraving spot. In order to avoid release of smoke (produced during the engraving process) into the working environment, the vent of the engraver was connected to an air filter (model AD350, BOFA; Staunton, IL), equipped with a HEPA/activated aluminum/potassium permanganate and an activated carbon panel.

A JEOL JSM-6150LV Scanning Electron Microscope (SEM, Peabody, MA) was used to take images of each of the selected substrates at 150x, 300x, 600x, and 1200x. In these cases, a Cressington sputter coater 108auto (Watford, Hertfordshire WD19 4BX, United Kingdom) was used to deposit a 15nm layer of gold on the substrate. Complementary 3D images were obtained using an opto-digital microscope (Olympus DSX-500, Center Valley, PA) and analyzed using the manufacturer's software package.

CorelDraw X6, by Corel Corp. (Ottawa, Canada), was used to design the  $\mu$ PADs as well as straight channels to measure the wicking linear velocity. The latter was investigated as a function of the channel width (in the 0.5 mm to 2.0 mm range) by analyzing the video data taken on 30 mm-long strips of paper and using a 10MP digital camera (at 30 frames per second, Canon PowerShot SX10 IS; Melville, NY).

## 2.5. Colorimetric Reaction and Analysis

In the presence of oxygen and water, glucose reacts with GOx in the detection zone to yield hydrogen peroxide. The H<sub>2</sub>O<sub>2</sub> is then reduced to H<sub>2</sub>O by horseradish peroxidase while iodide is oxidized to iodine concurrently producing the characteristic brown color.<sup>32</sup> For the experiments herein described, a 5:1 (v/v) solution of 645 units mL<sup>-1</sup> GOx and 339 units mL<sup>-1</sup> HRP was prepared in 100 mM phosphate buffer at pH 6.<sup>21</sup> A mixture of 0.6 M KI and 0.3 M trehalose was also prepared in 0.1M phosphate buffer at pH 6, to serve as colorimetric probe and enzyme stabilizer,<sup>21</sup> respectively. A 100 mM stock solution of glucose was prepared in buffer and used to prepare standard solutions by dilution in buffer. Different

<sup>2</sup>Due to the potential risk of fire, laser engravers should not be operated unattended.

volumes of reagents were tested on the paper chips. In all cases, the detection zone of the paper was spotted with a selected volume of the solution containing the GOx/HRP mixture and allowed to settle for 15 minutes in a humid environment at room temperature (petri dish contained 100% relative humidity). Next, the detection zone was spotted with the same volume of KI/trehalose and preserved in a humid environment for an additional 15 minutes at room temperature. Then, 7  $\mu$ L of a solution containing 20 mM glucose was pipetted at the base of the  $\mu$ PAD and allowed to travel through the paper (via the hydrophilic channels) to the detection zones. This concentration of glucose was selected because it is within the clinically relevant range for the analysis of glucose in plasma (2.5–50 mM<sup>1</sup>). The chip was finally set at room temperature for additional 30 min to allow the color development in the detection spot. Lastly, a color image was taken on a Canon CanoScan LiDE 700F scanner (Melville, NY) and analyzed using Adobe Photoshop CS6 (San Jose, CA). In all cases, a 5 mm-diameter detection zone was used to measure the mean color intensity (arbitrary units, AU) and standard deviation (used to quantify the color gradient). It is important to note that the  $\mu$ PADs were very sensitive to both temperature and humidity. Therefore, the use of ovens (that could dry the reagents and sample quicker but denature the enzyme) was avoided. Instead, the chips were maintained inside a petri dish (room temperature) during the duration of the experiments.

### 3. Results and Discussion

#### Characterization of the selected substrates

One critical parameter in the experimental design selected for these experiments is the topography of the substrates. In order to complement the data provided in Table 1, the topography of the six substrates was investigated using optical microscopy and SEM. Rather than tuning the fluid distribution rates to implement multiple assays in a single device,<sup>34</sup> the goal of these experiments was to gain insight about the size and distribution of the fibers in the surface of the paper. As it can be observed in Figure 1, significant differences were observed between filter and chromatography papers. While grade 1F is composed of fibers with an average dimension of  $19 \pm 1 \mu\text{m}$ , the average thickness of the fibers on grade 1 CHR chromatography paper is  $15 \pm 1 \mu\text{m}$ . Grade 3F has an average fiber size of  $15 \pm 1 \mu\text{m}$ , and grade 3MM CHR has fibers averaging  $10 \pm 3 \mu\text{m}$  in width. Whatman grade 4F consists of fibers  $20 \pm 4 \mu\text{m}$  wide, and grade 4 CHR has fibers measuring  $12 \pm 2 \mu\text{m}$ . These values were obtained by measuring the thickness of at least 20 fibers in the SEM image(see Supplementary Information). In general, each Whatman filter paper has thicker fibers than the parallel grade of chromatography paper. The thick fibers in the filter paper are used to form pores to trap solids. The percent difference between the thickest fibers on grade 4F ( $20 \pm 4 \mu\text{m}$ ) and thinnest on grade 3MM CHR ( $10 \pm 3 \mu\text{m}$ ) is 67.5%. Although these results are in agreement with the nominal data provided by the manufacturer, it is important to note that neither substrate displayed a pore size capable of trapping the reagents. Moreover, the hydrophilic nature of cellulose in its native form significantly impairs the possibility of using adsorption as a potential route of immobilization for the enzymes.

**Effect of channel dimensions on wicking velocity**—As previously mentioned,  $\mu$ PADs offer great freedom in terms of design, allowing the integration of elements with

different shapes,<sup>35</sup> patterns,<sup>14</sup> and sizes.<sup>1</sup> However, the characteristics of each paper (see Table 1) determine the wicking speed and could affect not only the contact time between the sample and the reagents but also the distribution of the reagents in the detection spot. Both of these issues can have an effect on the magnitude and homogeneity of the color. Therefore, the influence of the width of the channels on wicking velocity was first investigated. Figure 2 shows representative examples of the distance wicked by a blue dye aqueous solution when traveling in channels with different widths fabricated on grade 1 CHR paper.

As it can be observed, significant decreases in wicking speed were observed when using smaller channel widths as the solution moved through all the channels. This trend was attributed to an increase in resistance as the solution moves through the paper. In general, wider channels can provide lower resistance<sup>36</sup> and transfer the solution at a faster rate. Results collected with other substrates (see Supplementary Information) also showed similar trends (decreases in flow rate as the flow profile advanced through the device). Different grades of filter and chromatography paper provided both fast and slow flow rates when compared with each other (further details are shown in SI). In order to facilitate a rational selection of the substrate by other researchers, the wicking speed (mm/s) as a function of the channel width was calculated for the six selected paper substrates and fitted with a simple exponential decay function (see Figure 2A–D, Supplementary Information and SI Equation 1). Therefore, and although only slight differences were obtained, the decay constant obtained (for wicking speed as a function of distance) allows ranking the filter papers in decreasing order of wicking speed as grade 4F > grade 1F > grade 3F and the chromatography as grade 4 CHR > grade 1 CHR > grade 3MM CHR. These results are important for the rational selection of the substrate, the channel length, and to optimize conditions for applications where a timer or adequate control of the reaction time is required.<sup>4</sup>

**Color Intensity and gradient**—Using a calibration curve, the intensity of the color developed in the detection spot can be used to calculate the concentration of a given analyte in the unknown sample.<sup>8, 20, 25–27, 35, 37</sup> In most cases, the detection is based on reflectance (amount of light reflected off the testing zone) and is performed with a camera<sup>25</sup> or scanner.<sup>35</sup> For the experiments herein reported, the  $\mu$ PADs were scanned 30 min after adding the sample, when the color was fully developed. In all cases, 5.0 mm circular detection zones were used. This size was selected because it is the smallest detection zone in which a standard 0.5  $\mu$ L micropipette can accurately dispense a volume of reagent that is fully contained in the testing zone and does not flow into the channels.

Therefore, and according to the hypothesis, the effect of solution volume (spotted on the detection zone) on the signal magnitude and homogeneity was investigated for all selected papers. The results are summarized in Figure 3. In general, it can be observed that same grades of filter and chromatography paper rendered similar results in terms of signal intensity and uniformity. It was also observed, however, that these parameters were highly dependent on the volume of solution spotted in the detection zones. As it can be observed in Figure 3A, increasing the volume of reagents spotted in the detection zone can produce significant improvements (up to 143% using grade 1 CHR) in the signal magnitude (color intensity). This finding was attributed to the improved production of  $\text{H}_2\text{O}_2$  due to the

increased amount of enzyme available.<sup>38</sup> In this regard, it is important to note that grade 1 (either filter or chromatography) paper produced the highest color intensity in the studied range of volumes selected for these experiments.

It is also important to note that the increases in intensity produced by larger volumes of reagents were accompanied with systematic decreases in the color gradient observed across the detection spot (Figure 3B). While all substrates followed this trend, grade 1 CHR, the thinnest paper, yielded the highest gradient ( $40 \pm 10$  AU) when spotted with 0.5  $\mu$ L and showed the lowest gradient ( $7 \pm 1$  AU) when spotted with 1.0  $\mu$ L. The importance of these results is that the criteria to select the “best” paper for a particular application should be clearly stated. Furthermore, the results show evidence that such analysis can be heavily influenced by the experimental conditions selected. In all cases, and based on the results shown in Figure 3, it is clear that a compromise between signal intensity and color uniformity exists and that this relationship is influenced by the properties of each type of paper selected.

We believe these results are the consequence of several factors affecting the distribution of enzymes on the  $\mu$ PADs. First off, it is clear that thicker substrates (grade 3F and grade 3 MM CHR) always yield poor signal intensity. A reason for this is that the detection method is mainly sensitive to the compounds present on the surface of the device, which is opaque. Also, the small color gradient observed for these substrates could be attributed to a poor signal/noise rather than a true uniform distribution of the signal. The main advantage of these materials would be their high wicking speeds. Based on this (and assuming that wicking speed is controlled), it is reasonable to assume that either grade 1F or grade 1 CHR papers can be generally considered ideal substrates to fabricate  $\mu$ PADs. However, the large color gradient observed in these cases can be attributed to the poor affinity of proteins (GOx in this case) for the cellulose fibers, which leaves them loosely bound to the surface of the  $\mu$ PADs. Therefore, unless the substrate is saturated, the enzyme can be displaced when the sample wicks through the paper causing an uneven distribution of the reagents, and therefore a color gradient. A simple solution to this problem is to find a balance between the dimensions of the  $\mu$ PAD, the type of paper selected, and the volume of reagents spotted.

### Analysis of Glucose

In order to demonstrate that an adequate selection of the type of paper as well as the experimental conditions can affect both color intensity and uniformity, the detection of glucose (7  $\mu$ L sample containing 20 mM glucose) was performed using  $\mu$ PADs prepared under different conditions. As it can be observed in Figure 4A, grade 3F paper (spotted with 0.5  $\mu$ L of reagents) yielded the lowest mean color intensity ( $25 \pm 4$  AU) and a fair gradient ( $14 \pm 1$  AU). These results, which are in agreement with those previously discussed, show that the thickness and retention ability of the substrate combined with an insufficient amount of reagents could have devastating analytical consequences. On the other extreme, Figure 4B shows that when the same volume of reagents (0.5  $\mu$ L) is spotted on grade 1 CHR paper, a much improved mean color intensity ( $123 \pm 7$  AU) and a significant gradient ( $40 \pm 3$  AU) are obtained. Finally, Figure 4C shows that when the adequate volume of reagents (1  $\mu$ L) is



spotted on grade 1 CHR paper, the mean signal intensity can be maximized ( $177 \pm 3$  AU) and the gradient minimized ( $7 \pm 1$  AU).

## 4. Conclusions

The experiments described in this communication aimed at evaluating the suitability of six grades of Whatman paper for the fabrication of  $\mu$ PADs. The results presented complement nominal data for the selected papers (provided by the manufacturer). According to the presented results, thicker substrates (grade 3 filter or chromatography papers) display a higher resistance to the flow, transfer solutions at much lower rates, and yield poor color development/reading. On the other hand, faster transfers and better analytical performance can be obtained with thinner substrates (grade 1 filter or chromatography papers). In this case, the fabrication conditions (amount of enzyme) can be optimized to saturate the surface of the cellulose fibers in the detection spots, maximizing color intensity and uniformity. According to the presented results, this simple (yet effective) approach can be used to overcome one of the most significant limitations of  $\mu$ PADs.

## Supplementary Material

Refer to Web version on PubMed Central for supplementary material.

## Acknowledgments

Financial support for this project has been provided in part by the University of Texas at San Antonio and the National Institutes of Health through the Research Centers at Minority Institutions (G12MD007591). E.F.M.G. gratefully acknowledges the scholarship granted from Conselho Nacional de Desenvolvimento Científico e Tecnológico (CNPq) and Instituto Nacional de Ciência e Tecnologia de Bioanalítica (INCTBio) – Science without borders program (Grant No.246903/2012-0).

## References

1. Martinez AW, Phillips ST, Butte MJ, Whitesides GM. *Angew Chem Int Ed*. 2007; 46:1318–1320.
2. Bai P, Luo Y, Li Y, Yu XD, Chen HY. *Chin J Anal Chem*. 2013; 41:20–24.
3. Pelton R. *TrAC, Trends Anal Chem*. 2009; 28:925–942.
4. Lutz B, Liang T, Fu E, Ramachandran S, Kauffman P, Yager P. *Lab Chip*. 2013; 13:2840–2847. [PubMed: 23685876]
5. Wu XE, Guo YZ, Chen MY, Chen XD. *Electrochim Acta*. 2013; 98:20–24.
6. Thom NK, Yeung K, Pillion MB, Phillips ST. *Lab Chip*. 2012; 12:1768–1770. [PubMed: 22450846]
7. Carrilho E, Phillips ST, Vella SJ, Martinez AW, Whitesides GM. *Anal Chem*. 2009; 81:5990–5998. [PubMed: 19572563]
8. Carrilho E, Martinez AW, Whitesides GM. *Anal Chem*. 2009; 81:7091–7095. [PubMed: 20337388]
9. Schilling KM, Lepore AL, Kurian JA, Martinez AW. *Anal Chem*. 2012; 84:1579–1585. [PubMed: 22229653]
10. Olkkonen J, Lehtinen K, Erho T. *Anal Chem*. 2010; 82:10246–10250. [PubMed: 21090744]
11. Li X, Tian J, Nguyen T, Shen W. *Anal Chem*. 2008; 80:9131–9134. [PubMed: 19551982]
12. Nie J, Zhang Y, Lin L, Zhou C, Li S, Zhang L, Li J. *Anal Chem*. 2012; 84:6331–6335. [PubMed: 22881397]
13. Fenton EM, Mascarenas MR, López GP, Sibbett SS. *ACS Appl Mater Interfaces*. 2008; 1:124–129. [PubMed: 20355763]
14. Nie J, Liang Y, Zhang Y, Le S, Li D, Zhang S. *The Analyst*. 2013; 138:671–676. [PubMed: 23183392]

15. Bhakta SA, Borba R, Taba M Jr, Garcia CD, Carrilho E. *Anal Chim Acta*.
16. Dungchai W, Chailapakul O, Henry CS. *Anal Chem*. 2009; 81:5821–5826. [PubMed: 19485415]
17. Yu J, Ge L, Huang J, Wang S, Ge S. *Lab Chip*. 2011; 11:1286–1291. [PubMed: 21243159]
18. Taudte RV, Beavis A, Wilson-Wilde L, Roux C, Doble P, Blanes L. *Lab Chip*. 2013; 13:4164–4172. [PubMed: 23959203]
19. Yetisen AK, Akram MS, Lowe CR. *Lab Chip*. 2013; 13:2210–2251. [PubMed: 23652632]
20. Klasner SA, Price AK, Hoeman KW, Wilson RS, Bell KJ, Culbertson CT. *Anal Bioanal Chem*. 2010; 397:1821–1829. [PubMed: 20425107]
21. Dungchai W, Chailapakul O, Henry CS. *Anal Chim Acta*. 2010; 674:227–233. [PubMed: 20678634]
22. Martinez AW, Phillips ST, Nie Z, Cheng CM, Carrilho E, Wiley BJ, Whitesides GM. *Lab Chip*. 2010; 10:2499–2504. [PubMed: 20672179]
23. Jokerst JC, Adkins JA, Bisha B, Mentele MM, Goodridge LD, Henry CS. *Anal Chem*. 2012; 84:2900–2907. [PubMed: 22320200]
24. Pollock NR, Rolland JP, Kumar S, Beattie PD, Jain S, Noubary F, Wong VL, Pohlmann RA, Ryan US, Whitesides GM. *Sci Transl Med*. 2012; 4:152ra129.
25. Martinez AW, Phillips ST, Carrilho E, Thomas SW, Sindi H, Whitesides GM. *Anal Chem*. 2008; 80:3699–3707. [PubMed: 18407617]
26. Ellerbee AK, Phillips ST, Siegel AC, Mirica KA, Martinez AW, Striehl P, Jain N, Prentiss M, Whitesides GM. *Anal Chem*. 2009; 81:8447–8452. [PubMed: 19722495]
27. Wang W, Wu WY, Wang W, Zhu JJ. *J Chromatogr A*. 2010; 1217:3896–3899. [PubMed: 20444459]
28. Cassano C, Fan ZH. *Microfluid Nanofluid*. 2013; 15:173–181.
29. Chen X, Chen J, Wang F, Xiang X, Luo M, Ji X, He Z. *Biosens Bioelectron*. 2012; 35:363–368. [PubMed: 22472530]
30. Coltro WKT, de Jesus DP, da Silva JAF, do Lago CL, Carrilho E. *Electrophoresis*. 2010; 31:2487–2498. [PubMed: 20665911]
31. Li X, Tian J, Shen W. *Anal Bioanal Chem*. 2010; 396:495–501. [PubMed: 19838826]
32. Abe K, Suzuki K, Citterio D. *Anal Chem*. 2008; 80:6928–6934. [PubMed: 18698798]
33. Gabriel EFM, Coltro WKT, Garcia CD. *Electrophoresis*. 2014 in press.
34. Noh H, Phillips ST. *Anal Chem*. 2010; 82:4181–4187. [PubMed: 20411969]
35. Martinez AW, Phillips ST, Whitesides GM, Carrilho E. *Anal Chem*. 2009; 82:3–10. [PubMed: 20000334]
36. Godwin LA, Deal KS, Hoepfner LD, Jackson LA, Easley CJ. *Anal Chim Acta*. 2013; 758:101–107. [PubMed: 23245901]
37. Li X, Tian J, Shen W. *Cellulose*. 2010; 17:649–659.
38. Mikkelsen, SR.; Corton, E. Vol. 3. John Wiley & Sons, Inc; 2004. p. 51-60.



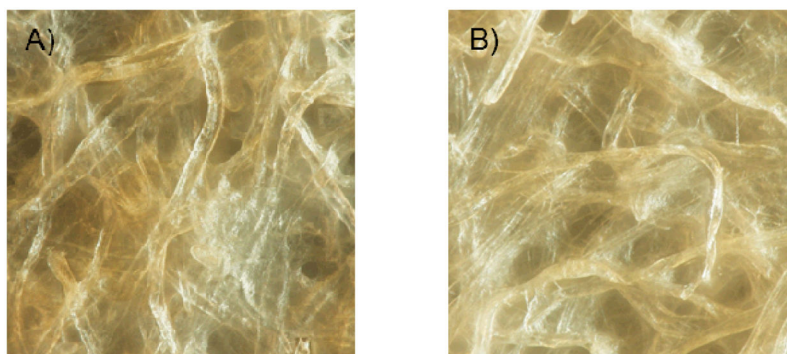


**Figure 1.**  
Surface topography of (A) grade 1 filtration and (B) grade 1 chromatography papers.

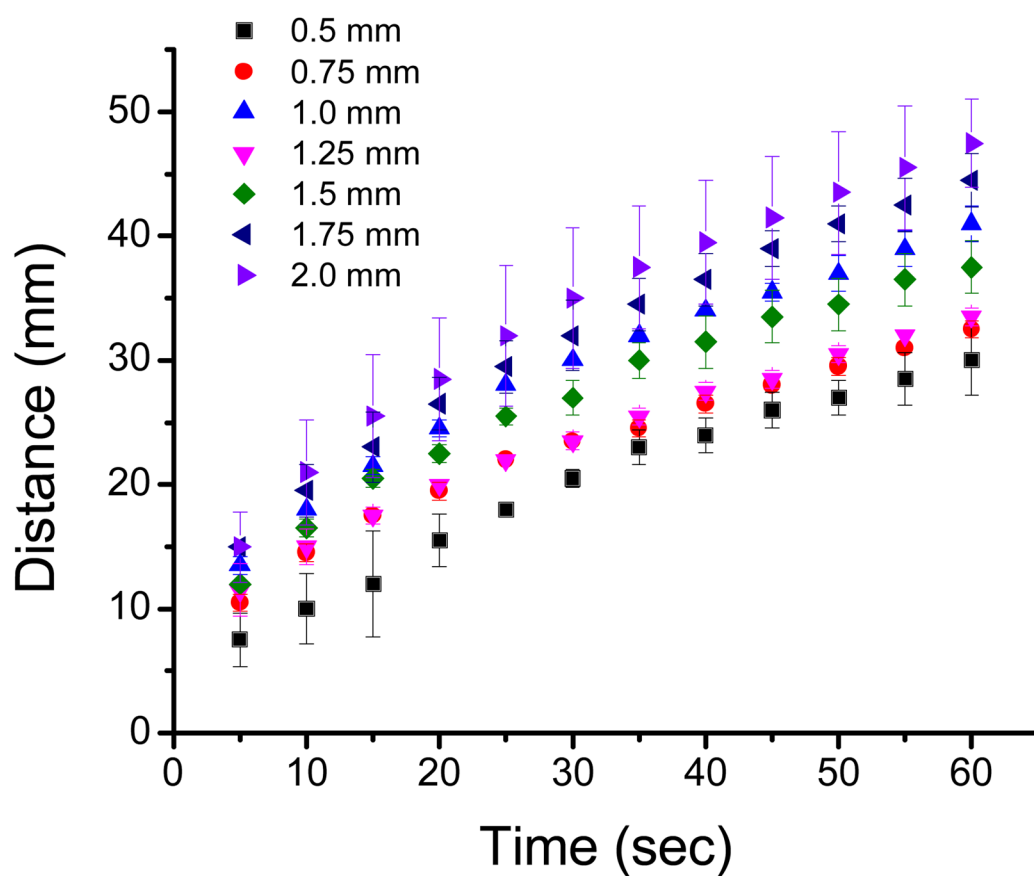


**Figure 2.**  
Distance travelled by an aqueous solution as a function of time for channels with different widths fabricated with grade 1 chromatography paper.

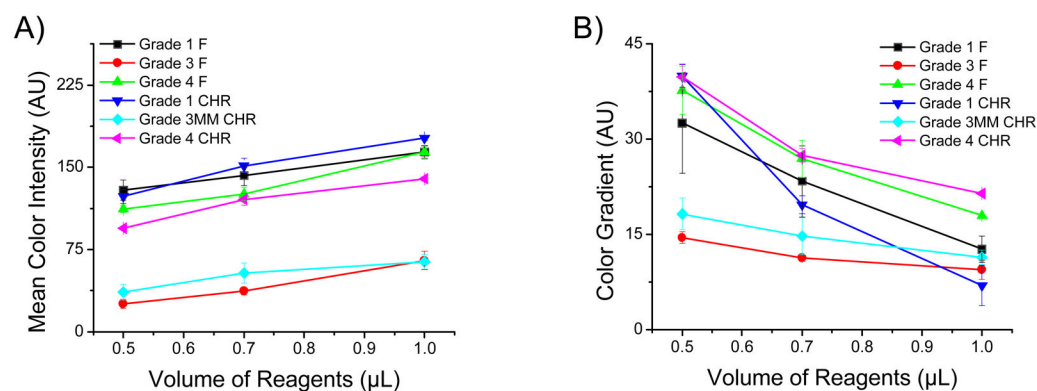


**Figure 3.**

The mean color intensity (A) and color gradient (B) as a function of different volumes of reagent (GOx/HRP and KI/Trehalose) – 0.5  $\mu\text{L}$ , 0.7  $\mu\text{L}$ , and 1.0  $\mu\text{L}$ . Data points and error bars correspond to the average and standard deviation obtained with at least three images. The color gradient was measured using the image's color standard deviation.

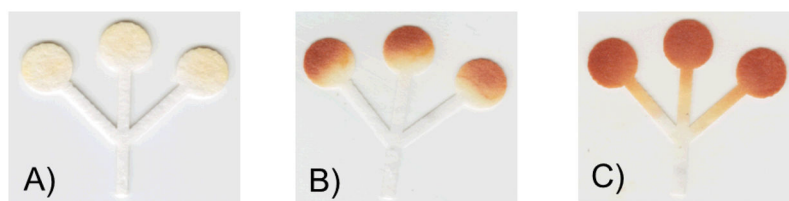


**Figure 4.**

Images displaying (A) the lowest color intensity (grade 3F), (B) the largest color gradient (grade 1 CHR), and (C) the best color intensity with the most uniformity (grade 1 CHR).

The color generated inside the channels (C) is attributed to excess color reagent spotted on detection zone.

Nominal specifications obtained for the substrates used to fabricate  $\mu$ PADs. N/A = data not available. The porosity value corresponds to nominal results collected using the Gurley method (air). Particle retention information corresponds to the cut-off rating at 98% efficiency. The filtration speed was determined by Herzberg method.

Table 1

	Qualitative Filtration				Chromatography			
	Grade 1	Grade 3	Grade 4	1 CHR	3MM CHR	4 CHR		
Weight (g/m <sup>2</sup> )	88	187	96	87	189	93		
Thickness ( $\mu$ m)	180	390	205	180	340	210		
Porosity (sec)	10.5	26	3.7	10.9	19.1	3.4		
Particle retention ( $\mu$ m)	11	6	25	11	6	20		
Filtration speed (sec/100mL)	150	2	37	N/A	N/A	N/A		
Wicking speed (mm/30 min)	N/A	N/A	N/A	130	130	180		